Ultraviolet-induced chemical vapor deposition of silica films studied by surface-sensitive multiple-internal-reflection spectroscopy

C. Licoppe and C. Debauche
Laboratoire de Bagneux (LA250), Centre National d'Etudes des Télécommunications, France Telecom, 196, Avenue Henri Ravera, Boîte Postale 107, 92225 Bagneux, France
(Received 20 April 1992)

Surface-sensitive multiple-internal-reflection-absorption infrared spectroscopy has been applied to the study of SiO_2 photodepostion under far-ultraviolet illumination. A Si-H absorption line at 2208 cm^{-1} is shown to characterize the surface incorporation site of silicon atoms. Evidence is given for its assignment to O_2SiH_2 molecular configurations. A previously overlooked silicon incorporation path involving surface photoexcitation of water sites and reaction with silane molecules is identified, and shown to account for about 5% of silicon atom incorporation. Infrared spectroscopic data provide evidence for kinetic roughening of the deposition front, and the measure of the β exponent gives a value of 0.28 ± 0.05, in fair agreement with theoretical and numerical predictions for ballistic and random deposition models.

I. INTRODUCTION

Ultraviolet-assisted chemical vapor deposition (UVCVD) of dielectric materials such as SiO_2 is increasingly as a low-temperature processing alternative to plasma-enhanced dielectric deposition techniques in device fabrication.[1] One can thus find SiO_2 films made from SiH_4/O_2 gaseous mixtures,[2] but also from SiH_4/N_2O,[3] SiH_4/NO_2,[4] SiH_4/CO_2,[5] Si_2H_6/O_2,[6] $Si_2H_6+(SiF_4$ or $Si_2F_6)/O_2$,[7] in all cases under ultraviolet irradiation. In view of the impressive collection of gaseous precursors from which silica film photodeposition was achieved, the understanding of the photodeposition mechanisms appears very limited indeed. It is nevertheless an appealing technique from a more fundamental point of view, because it constitutes a gas-surface deposition process which may operate at low temperatures where very little diffusion occurs, and also in conditions where the initial reactions are triggered by ultraviolet light with wavelength shorter than 200 nm, thus allowing for some amount of spectroscopic discrimination. Moreover, the UVCVD of SiO_2 will be shown here to involve only a relatively small number of bulk and surface chemical configurations, while other "cold" techniques such as plasma-enhanced chemical vapor deposition involve many bulk hydrogenated configurations.[8]

This relative simplicity allowed us, taking advantage of the surface sensitivity reached by *in situ* multiple-internal-reflection infrared spectrometry,[9] to analyze the surface sites involved in the photoinduced incorporation of surface species into the deposition front. In particular, we identify the absorption line of the silane photochemisorption site, which we assign to an O_2SiH_2 molecular configuration, and find a new mechanism for photoassisted silicon incorporation without any oxidizing species in the gas phase.

The study of kinetic growth phenomena has been a very active research area in the recent years.[10] In the last part of our paper we argue for the relevance of low-temperature silica photodeposition as an experimental realization of ballistic deposition. More precisely, we show by relying on the quantitative estimate of surface species provided by our infrared-absorption technique the occurrence of kinetic roughening of the deposition front, and we determine experimentally the value of the characteristic β exponent for deposition front roughening. We eventually argue for a possible transition in the deposition mode from ballistic towards random deposition with increasing substrate temperature.

II. EXPERIMENT

The experimental apparatus is composed of a rapid thermal chemical vapor deposition (CVD) vessel,[11] equipped with low-pressure mercury lamps providing UV lines at 185 and 254 nm and coupled to a modified Nicolet 740 SX spectrometer through ZnSe windows. CVD occurred on the upper side of a semiconductor prism cut into a rectangular shape, 50 mm long, 5 mm wide, and 1 mm thick with both edges bevelled at 45°. This experimental geometry allows for about 40 total internal reflections on each face. The sensitivity of the system is $\Delta R/R = 5\times10^{-5}$ at 2000 cm^{-1} with 1000 scans of the interferometer, so that 0.02 layers of SiO_2 could be detected on InP. Data are taken in unpolarized light with a resolution of 4 cm^{-1}.

Heating of the substrate is due to irradiation by a row of halogen lamps located below the sample, according to a standard rapid thermal processing setup. Temperature was determined by means of a thermocouple imbedded in a 300-μm-thick silicon wafer replacing the internal refection element. For temperatures below 300 °C, this procedure provides an absolute determination of temperatures for the general case within 50 °C with main uncertainties due to heat losses in the cement holding the thermocouple and the different reflectivities of Si, InP, and Ge. The temperatures obtained in a given experimental setup during consecutive deposition runs are however reproducible within 2 °C. For deposition runs lasting

more than 10 s and less than 15 min, lamp cycles were adjusted so as to keep thermal drift within ±2 °C, therefore ensuring a constant deposition temperature.

In most experiments reported below, the multiple-internal-reflection element was made of iron-doped semi-insulating InP. Prior to the experiments, the InP wafer was chemomechanically polished in a solution of bromine in methanol and thoroughly rinsed in de-ionized (DI) water. X-ray photoemission spectroscopy (XPS) measurements performed in a ultrahigh-vacuum (UHV) chamber with a base pressure of 10^{-11} Torr were used to characterize the wafers after the cleaning procedure and calibrate film thicknesses. The UVCVD vessel and the UHV chamber are not connected. Hence the samples were exposed to air prior to their introduction in the XPS analysis chamber. This leads to a slight dehydrogenation and reoxidation of the deposited SiO_2 films, but it has no consequence on the silicon atom coverage whose value is used here for calibration purposes. The cleaning procedure leaves about two monolayers of InP native oxide at the surface. This layer may react with silane to produce an ultrathin silica layer on top of the wafer, but this reaction is slow enough to be negligible in a real deposition experiment.[12] To determine film thicknesses with XPS, the integrated area of the Si($2p$) XPS peak located at 103.5 eV in SiO_2 was converted to coverage values by comparison with InP and SiO_2 standards assuming usual values for escape depths.[13] An upper limit of ±20% error can be assigned to this quantitative determination of coverages. In the following, the number of atoms in a monolayer will be taken at its value on the InP surface, that is 4.8×10^{14} atoms/cm^{-2}. The total integrated infrared absorption in the Si-O antisymmetrical stretch region (1000–1270 cm^{-1}) correlated linearly with the integrated area of the Si XPS line and film thicknesses could thereon be estimated from infrared spectra only. It was experimentally observed that the linearity in the infrared-absorption measurement persisted up to thicknesses of 200 Å

The long-wavelength transmission drop due to absorption by the InP phonon combination bands prevented the observation of absorption bands with wave numbers below 1000 cm^{-1}. In some experiments where the observation of Si-H bending modes in the region extending between 850 and 1000 cm^{-1} proved to be essential, an undoped germanium wafer was used instead. After degreasing with the usual tricholoroethylene-acetone-methanol sequence, the wafers were treated with the following desoxidizing procedure:[14] 1:1:4HCl(38%):H_2O_2(30%): DI water for 5 min, DI water rinse, then H_2O_2(30%) for 5 min, DI water rinse, 1:10HF(48%):DI water until hydrophobic (about 2 min), and a final DI water rinse.

Photochemical deposition of SiO_2 was achieved at temperatures between room temperature (RT) and 200 °C. At these temperatures, purely thermal CVD was observed to be negligible, so that the deposition parameters are controlled by photochemical processes. Growth runs were performed in a N_2:O_2:SiH_4 mixture under UV irradiation with flow rates 500:100:5 SCCM (SCCM denotes cubic centimeter per minute at STP) and a total pressure of 10 Torr unless specified otherwise. We observed deposits due in part to gas-phase nucleation on the wafer at a silane flow value of 10 SCCM. This threshold was independent of the wafer temperature in the range investigated here, so that by choosing a working flow value of 5 SCCM, we kept deposition parameters in the range where deposition is controlled by gas-surface processes. The purpose of the following two sections will be to compare the structure of photodeposited SiO_2 films at both temperatures with the help of the infrared data.

III. THE Si-O STRETCHING ABSORPTION AND THE STRUCTURE OF PHOTODEPOSITED, ULTRATHIN SILICA FILMS

Figure 1 shows the differential infrared spectra observed after several runs at RT and 200 °C in the region of the Si-O stretching resonances. Each spectrum in Fig. 1 must be interpreted as a balance between what was substracted from the previously deposited layer. At 200 °C [Fig 1(a)], the 20 s run duration was chosen so as to deposit reproducibly four monolayers of SiO_2 with each run. These film thicknesses were derived from the integrated intensity of the Si-O stretching band. In this regime of very slow deposition rates, no transitory pattern in the composition of the film was observed as is the case with faster deposition kinetics.[15] Figure 1(b) shows the spectra obtained in the room-temperature runs. In the monolayer range at RT, deposition rates increased with each run; run duration was chosen at 3 min in which case the first four runs led to deposits increasing from two to six monolayers.

Contrary to the high-temperature case, films grown at room temperature exhibited porosity and surface roughness. This is seen from the high level of absorption in the 1100–1200 cm^{-1} region, which has been assigned to disorder-activated modes,[16] and which systematically correlated in our experiments with (i) a high density of

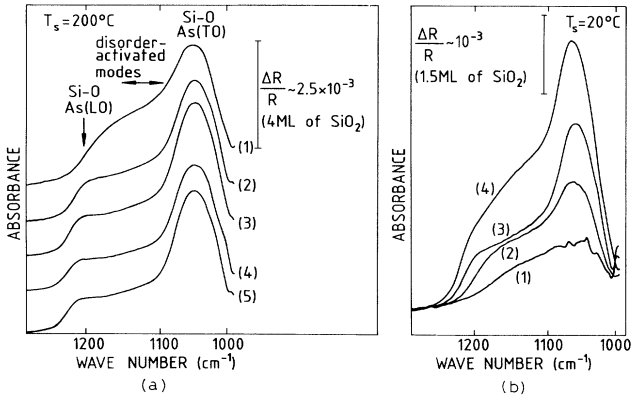

FIG. 1. Multiple-infrared-reflection-absorption spectra in the Si-O stretching region for consecutive UVCVD deposition cycles of SiO_2 performed at 200 °C (a) and room temperature (b). Spectra are indexed according to the sequence of deposition cycles. Spectrum n shows the difference in the absorbance spectrum between the sample after n deposition cycles and the sample after $n-1$, thus figuring the specific contribution of the nth deposition cycle to the infrared absorbance.

Si-H bonds which locally terminates the amorphous network, (ii) a rough surface morphology in scanning electron microscopy, and (iii) electrical leakage in the case of thicker layers. Therefore, RT photodeposited silica have a high degree of porosity, meaning a higher surface-to-volume ratio than films deposited at higher temperatures.

IV. INFRARED ABSORPTION IN THE Si-H REGION AND THE ORIGIN OF THE Si-H ABSORPTION LINE AT 2208 cm^{-1}

Figure 2 shows the differential infrared spectra observed after 5 runs in the region of the Si-H stretching resonances, with different substrate temperatures. Two distinct absorption peaks can be observed at 2260 and 2208 cm^{-1} with a constant full width at half maximum (FWHM) of 50 cm^{-1}. The peak at 2260 cm^{-1} is a regular feature of hydrogen-containing SiO_2 films: it is assigned to the hydrogen stretching of a O_3Si-H unit in a SiO_2 matrix. Its frequency is shifted to high energies relatively to the 2000 cm^{-1} line associated to the stretching mode of a Si-H bond in an a Si:H matrix because of the induction effect due to the stronger electronegativities of the backbonding oxygen atoms.[17] The intensity of this band correlates with that of the Si-O stretching absorption band, which is characteristic of a defect scattered in the bulk of the films. The density of such hydrogen groups in the film decreases at with higher substrate temperatures, as previously observed in thicker films.[18]

The other line observable in the Si-H stretching region is located at 2208 cm^{-1}. Its FWHM is also 50 cm^{-1} which is narrow enough to assign it to a single molecular configuration. It has not been reported before within the limits of our knowledge. With our highly sensitive absorption experiments we have systematically observed its appearance in photodeposited silica films, if sometimes in submonolayer amounts. It will be shown here to be produced by the photoinduced chemisorption of silane. For growth runs performed at 200 °C [see inset in Fig. 1(a)], this specific feature disappears after the first run in the differential spectra of the new material added by following growth runs. The possible reasons are the following: either it is related to an interface bonding configuration which additional SiO_2 covers without removing, or its related to an interface bonding state of the growing overlayer. The hypothesis of a buried interfacial layer is inconsistent with the room-temperature data, where it keeps being produced over thicker films. On the other hand, the surface site hypothesis fits the observations that porosity and surface roughness lead to an increase in the surface-to-volume ratio as the decomposition proceeds with a regular addition of active surface sites, and therefore to the persistence of the corresponding surface line at 2208 cm^{-1}. Moreover, this vibration surface peak was not observed in the layers grown at 200 °C by a purely thermal process with longer exposure times. In the case of single-gas treatments, it could not be observed in any case whatsoever, unless the UV light source was turned on. This line is therefore associated to a surface site whose production is directly related to UV irradiation.

The photoinduced reaction of silane with the deposition surface leads to the appearance of this specific absorption band, as shown by the experiments described in Fig. 3. These experiments use the sensitivity of the multiple-internal-reflection technique by detecting the surface modifications induced by exposures to a single gas under UV irradiation. A film grown at room temperature is thus simultaneously exposed twice to oxygen and UV light. The Si-H bonds vibrating at 2208 cm^{-1} are about five times more reactive to photoexcited oxygen than those at 2260 cm^{-1}, and they disappear preferentially during oxygen exposures as curves *a* and *b* of Fig. 2 show. After these treatments which remove three quarters of

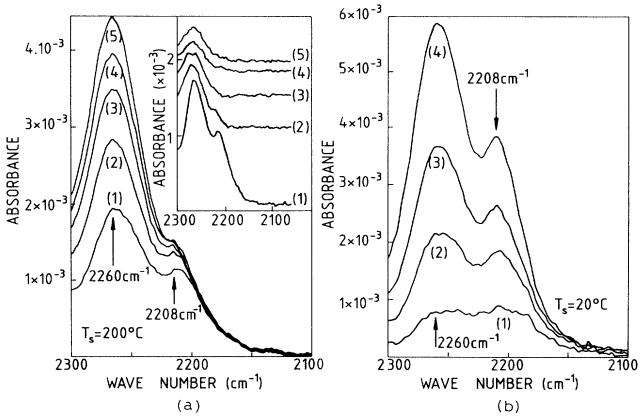

FIG. 2. Multiple-infrared-reflection-absorption spectra in the Si-H stretching region for consecutive UVCVD deposition cycles of SiO_2 performed at 200 °C (a) and room temperature (b). Spectra are indexed according to the sequence of deposition cycles. The inset in (a) shows differential spectra that isolate the single contribution of the *n*th deposition.

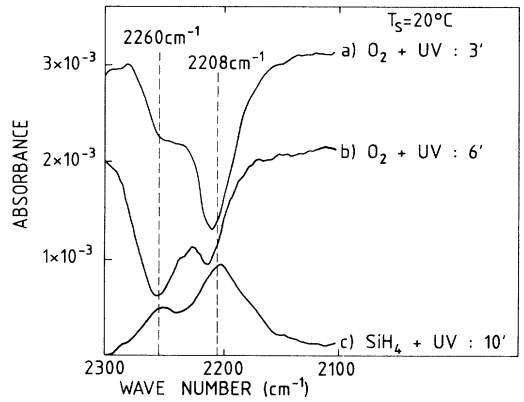

FIG. 3. Modifications in the Si-H region of the absorbance spectrum of an as-grown ultrathin silica film due to specific gaseous treatments. These were all performed at a pressure of 2 Torr and at room temperature. As in Fig. 1, positive absorbance peaks mean addition of Si-H bonds, while negative peaks indicate removal of such bonds during the treatment. In the sequence of treatments described here, the sample was exposed to oxygen and UV irradiation for 3 min (curve *a*) and then again at 6 min (curve *b*), and to silane and UV irradiation for 10 min (curve *c*), figuring at last an addition of Si-H bonds.

the 2208-cm^{-1} band, the surface is exposed to silane and UV light, and an increase of the peak at 2208 cm^{-1} is observed (curve *c*). This sequence involving oxygen and then silane exposures is the only one that leads to a net increase in the peak at 2208 cm^{-1}. By contrast with the 2260-cm^{-1} Si-H line, which can be produced by heating the film in a neutral ambient and thus is also due to intrasurface reactions, the 2208-cm^{-1} line therefore characterizes a photochemisorption site of silane, resulting only from gas-surface processes. We can estimate the number of such sites, for instance on the surface of the film grown at 200 °C in Fig. 1(a), by using previous calibrations of infrared data:[19] if the molecular unit giving rise to the Si-H line involves *n* Si-H bonds, this number is $4/5n$ monolayers. Since *n* can be 1, 2, or 3, it is clear that a significant fraction of the growth surface is covered by photochemisorbed silane.

V. IDENTIFICATION OF THE MOLECULAR CONFIGURATION RESPONSIBLE FOR THE ABSORPTION BAND AT 2208 cm^{-1}

Isotropic experiments are currently used for an unambiguous infrared line assignment. However the use of deuterated silane or O_2^{18} is quite expensive in flow mode in a CVD reactor. We will show here how it is possible to lift many uncertainties by paying close attention to the joint behavior of stretching and bending vibration modes, without requiring costly additional isotopic experiments.

To obtain additional data on the surface site characteristic of silane incorporation, we have explored the low-frequency region of the spectrum (850–1000 cm^{-1}) by working with germanium wafers prepared as described above. An additional constraint to obtain data on surface sites absorption bands in this region is to work with ultrathin layers, that is with thicknesses below 3 monolayers (ML), to ensure that the intense bulk absorption peaks due to Si-O stretching modes whose low-frequency side extends down to 980 cm^{-1}, and Si-OH bending modes at 940 cm^{-1} do not wash the weaker surface peaks out. An example is provided in Fig. 4, which shows the absorption spectra taken during the progressive deposition of one monolayer of silica on the germanium wafer.

Two peaks may be identified in the bending mode region. The peak observed at 880 cm^{-1} correlated systematically with the O_3Si-H absorption at 2260 cm^{-1}, in agreement with previous data, and supporting an assignment of this line to the bending mode of an O_3Si-H group in a silica matrix.[20] A second absorption peak is observed around 975 cm^{-1}, which correlates with the signal at 2208 cm^{-1}. A similar line has been observed in plasma-deposited films, associated to a companion peak at about 935 cm^{-1}, which has been, respectively, assigned to $(SiH_2)_n$ scissor and wagging modes, displaced from their 890 and 845 cm^{-1} value in polysilane alloys[21] by the induction effect in the SiO_2 medium. In our experiments with the low-pressure mercury lamp, we could not see any significant absorption around 940 cm^{-1}. In some deposition experiments we have used a rare-gas pulsed flash lamp developed in our laboratory,[22] with a wide-band UV emission in the region between 170 and 250 nm,

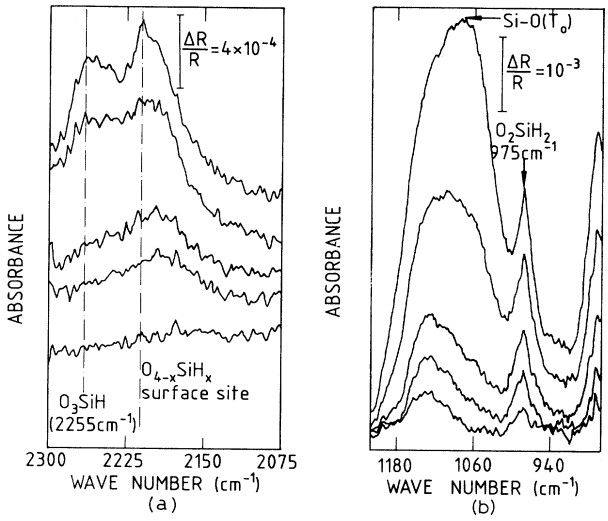

FIG. 4. Progressive buildup of one monolayer of silica on germanium at room temperature with a low-pressure mercury lamp. The gas-flow values of the $N_2/O_2/SiH_4$ system were set at 500:100:5. Exposures were performed in the following order: 3 min at 5 Torr, 3 min at 5 Torr, 5 min at 5 Torr, 3 min at 10 Torr, and 5 min at 10 Torr. The spectra shown on the figure were taken after each exposure step. (a) reports the absorption spectra in the Si-H stretching energy region. (b) reports the same spectra in the Si-O stretching and Si-H bending energy region.

and an integrated UV luminance about 10 times more intense than with the standard low-pressure mercury lamps used in all the experiments reported above.

Figure 5 shows the infrared-absorption spectra due to sequential deposition of silica at room temperature assisted with this lamp, from a few monolayers up to 100 Å. It features a stronger absorption signal at 2208 cm^{-1} than in similar films prepared with the mercury lamps. The spectra then clearly feature the doublet at 975 and 935 cm^{-1}. Figure 6 shows the correlation between the intensities of the stretching mode at 2208 cm^{-1} and that of these two modes at lower energies obtained on several experiments. In spite of some dispersion in the data due to the difficulty to draw a baseline in this region of the spectrum, the correlation between these modes appear clearly. Therefore the line at 2208 cm^{-1} may be assigned to the stretching vibration of hydrogen in surface O_2SiH_2 groups.

To reconcile the variations in the occurrence of the full bending mode doublet, it must be noted that in the scissor mode of the SiH_2 unit, the hydrogen atoms are moving while the silicon keeps almost at rest. On the other hand in the wagging mode, the silicon atom experiences a significant displacement. Hence this mode is more sensitive to the environment of the silicon atom. Its shift in frequency when going from isolated SiH_2 groups to $(SiH_2)_n$ is much greater than the scissorlike mode, as shown by theoretical calculations.[21] It is then plausible to think that is appears at 935 cm^{-1} only during deposition

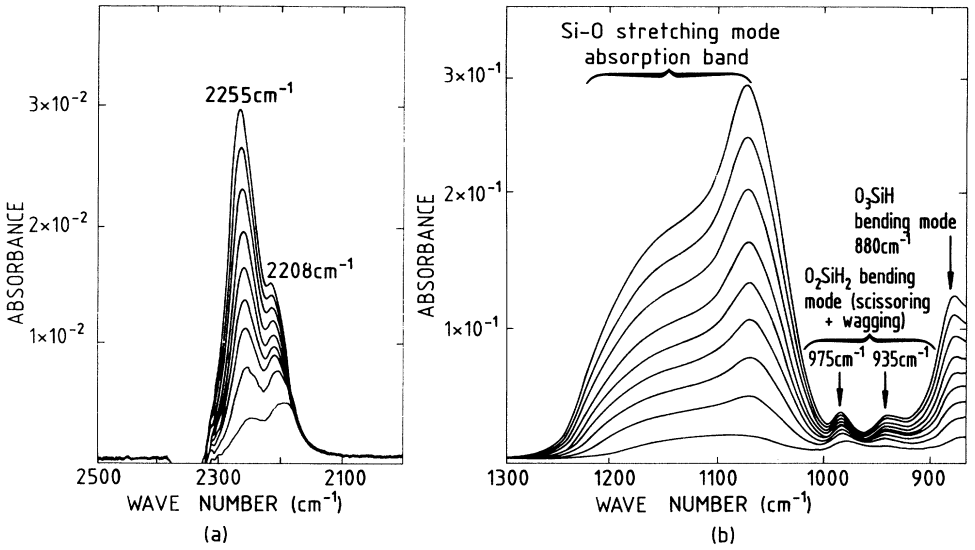

FIG. 5. Progressive buildup of a 100-Å-thick layer of silica deposited at room temperature and a total pressure of 10 Torr with a pulsed xenon lamp operating at 2 Hz, featuring the Si-H stretching modes (a) and the Si-H bending modes (b).

at high-UV flux, where the amount of SiH_2 groups is greater. The bending modes are a very sensitive tool to distinguish between different deposition front environments, and more work is clearly needed to move beyond this assignment towards an identification of the environment of these groups, for example at the level of next-to-nearest neighbors, but even in its limited form it will allow to proceed in the analysis of the deposition mechanisms.

We have assigned the molecular configuration O_2SiH_2 to the surface site produced after silane photochemisorption. But silane does not absorb UV light at 185 and 254 nm in the gas phase.[23] This has been one fundamental tenet of the current understanding of UVCVD deposition of SiO_2 films. The chemisorption of silane may be photoactivated though, as shown above. Hence photoactivation of silane can occur at the surface, and it becomes important to identify the surface site involved in the photochemisorption of silane molecules.

VI. ADSORBED WATER IN THE SURFACE REACTIONS

To understand what types of sites on the surface are active for photochemisorption, a convenient starting point is the observation that photoinduced chemisorption of silane could only be observed after exposures of the films to photoexcited oxygen at room temperature. Gas-phase photochemistry studies[24] have demonstrated the high reactivity of Si-H features to photoexcited oxygen and its capacity to break Si-H bonds and produce hydroxyl groups. The absorption spectra in the 3000–4000 cm^{-1} spectral region are shown in Figs. 7(a) and 7(b) for the sequence of photodepositions of Figs. 1(a) and 1(b), respectively. When deposition cycles are performed at 200 °C, Fig. 7(a) shows the continuous incorporation of water and Si-OH groups. On the other hand, when deposition cycles are performed at room temperature, the spectra evolve significantly during the first cycles. In the first cycle it shows the absorption band for undissociated adsorbed water, and each deposition cycle shows additional absorption on the high-energy side of this band, corresponding to increasing amounts of dissociated water groups and Si-OH bonds, until the spectrum looks like those obtained in Fig. 1(a). This shift suggests that adsorbed water is produced at the surface by the photodeposition process in a stationary manner, while increasing amounts of Si-OH groups and dissociated water which are by-products of surface reactions will remain in the bulk of the films.

To check on this view, a freshly deposited film with thickness 20 Å was heated at 300 °C for 30 min under nitrogen flow so as to remove all the absorption due to bulk OH groups, and be in a position to detect OH-related absorptions due to surface effects. This film was then exposed under UV irradiation to oxygen and then to silane.

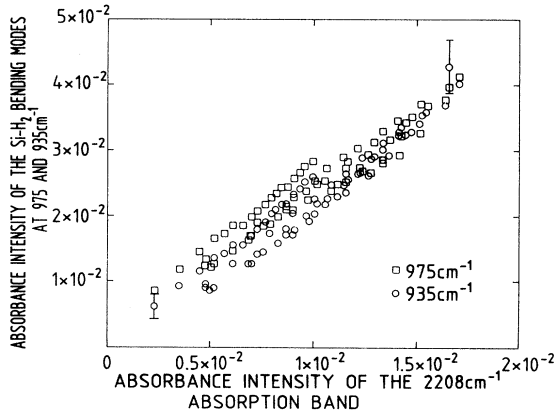

FIG. 6. Correlation of the intensities of the Si-H stretching mode at 2208 cm^{-1} with that of the doublet at 975 and 940 cm^{-1}, for a set of silica photodeposition sequences performed with the pulsed lamps. The relative translations of the curves corresponding to different experiments are due to the difficulty to draw a baseline in the lower energy region of the spectra where different peaks overlap.

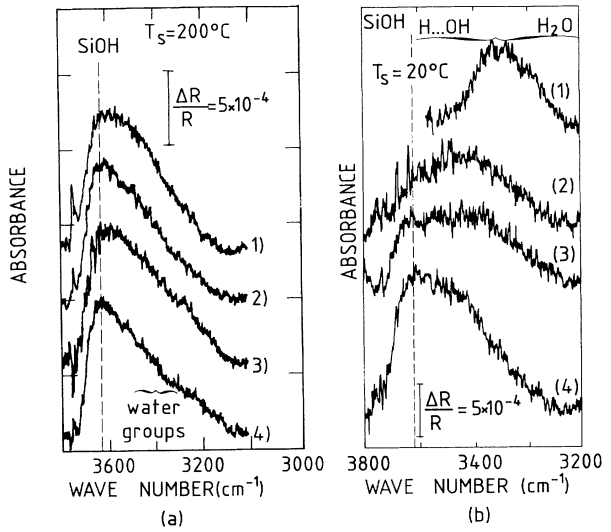

FIG. 7. Multiple-infrared-reflection-absorption spectra in the O-H stretching region for consecutive UVCVD deposition cycles of SiO_2 performed in the same series of experiments as in Fig. 1: (a) shows the deposition sequence at 200 °C and (b) that performed at room temperature.

The behavior of the Si-H features in the spectra was similar to that reported in Fig. 3, and that of the OH-related absorption band is reported in Fig. 8(a). Curve *a* shows an increase in the signal around 3350 cm^{-1} which is usually attributed to water. The overall behavior in the gas-surface photochemistry thus agrees with the conclusions of gas phase studies, with conversion of some Si-H features into OH-containing groups. Curve *b* in Fig. 8(a) shows that the subsequent silane exposure consumes O-H bonds. As shown in a parallel experiment, this consumption cannot be accounted for by UV irradiation alone, which acts much more slowly on the OH bonds.

By carefully heating the film before performing the oxygen and silane exposure sequence, it becomes, therefore, possible to visualize the surface creation of hydroxyl and their consumption in the silane photochemisorption process. The integrated absorbance of the Si-H signal at 2208 cm^{-1} added during the silane photoexposure is plotted in Fig. 8(b) as a function of the integrated absorbance of the O-H bonds which disappear during the same exposures. As expected, a linear relationship is obtained. Taking a standard attenuation coefficient in silica glasses of 77 mol cm/l,[25] 0.55 ML of surface water groups are consumed in order to produce 0.4 ML of photochemisorbed silane. In view of the uncertainties of the calibration data on the OH absorption bands, this is quite consistent with the assumption that silane photochemisorbs on OH-related sites, breaking one or two water groups at a time.

We have thus isolated a new photoactivated surface reaction in which silane reacts with surface water groups and gets incorporated into the film under the form O_2SiH_2. If silane does not react with ultraviolet light at these wavelengths, water is known to show intense ultraviolet absorption between 140 and 190 nm due to the X^1A_1-A^1B_1 transition,[26] so that it may account for the enhancement of silane incorporation by UV irradiation. Moreover, the surface reaction kinetics are such that with a pressure of 2 Torr of silane, half the number of reactive sites is burnt in 3 min at room temperature. Since the deposition rates for SiO_2 films increase linearly with silane partial pressure and that this parameter in the deposition experiments was about 0.1 Torr, it can be estimated that this new surface mechanism accounts for about 5% of the incorporation of silicon atoms in the films, and probably less at higher temperatures where part of the water desorbs from the deposition front, so that silane incorporation mechanisms must be understood mainly from a picture of gas-phase kinetics to which we will turn now. But it must be pointed that the existence of a significant photochemisorption mechanism for silane is important in current topics of interest such as semiconductor-dielectric layer interface preparation[27] and layer-by-layer UV photodeposition of silica films.[28]

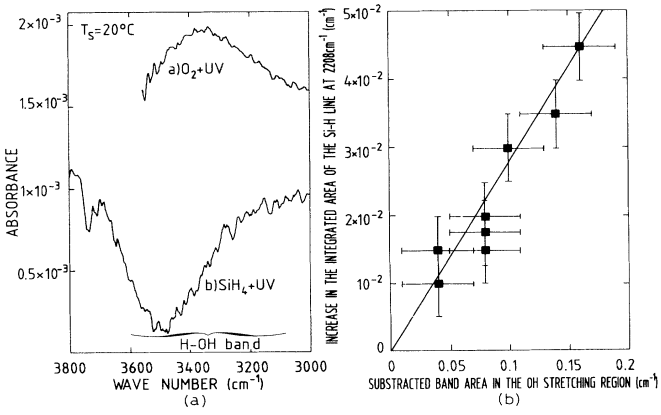

FIG. 8. (a) Differential spectra in the OH region of an annealed SiO_2 deposit following O_2+UV exposure and then SiH_4+UV exposure. (b) Integrated absorbance of the OH groups vs integrated absorbance of the Si-H 2208 cm^{-1} line for increasing SiH_4+UV exposures of this annealed SiO_2 deposit.

VII. REACTIONS IN THE GAS PHASE

We will try in this section to write down and discuss a basic system of chemical equations. The aim of this section is to obtain a qualitative picture of what is going on in the gas phase, so as to try to devise a mechanism for silicon dioxide deposition under ultraviolet irradiation incorporating the minimal features necessary to account for our data. These reactions and their rates are derived from the collection of data by Baulch and coworkers.[29] The primary photolysis involves a breakdown of the oxygen molecules by the photons with a wavelength of 185 nm,

$$O_2+h\nu(185\text{ nm})\rightarrow 2O(^3P)\text{ with }\sigma_1=1.61\times10^{-20}\text{ cm}^{-2}\,. \quad (1)$$

Atomic oxygen is able to break silane molecules, a reac-

tion to which photochemists have paid some attention lately,[25] and oxygen molecules, themselves to produce ozone,

$$O(^3P)+SiH_4 \rightarrow OH+SiH_3 \quad \text{with } k_2=1.4\times10^{-12}\ \text{molec}^{-1}\times\text{cm}^3\times\text{s}^{-1}, \tag{2}$$

$$O(^3P)+O_2+M \rightarrow O_3+M \text{ with } k_3=6.9\times10^{-34}[O_2] \quad \text{if } M=O_2 \text{ or } 6.2\times10^{-34}[O_2] \text{ if } M=N_2 . \tag{3}$$

Ozone may be dissociated into atomic oxygen by the second ultraviolet line of the low-pressure mercury lamp at 254 nm, a reaction path which has been argued to be important in photoinduced deposition of SiO_2.[30] Using the kinetic data given here, it is easy to compare the rates in both paths and eliminate the unknown concentration $[O^3P]$ in the ratio,

$$\frac{\nu_{\text{ozone}}}{\nu_{\text{silane}}}=\frac{k_3[N_2][O_2]}{k_2[SiH_4]} . \tag{4}$$

At the low pressures used here this ratio is about 0.002, so that the reaction path leading to ozone formation can safely be neglected.

The creation of OH radicals leads to a set of secondary reactions and photolyses,

$$O(^3P)+OH \rightarrow O_2+H \text{ with } k_4=3.3\times10^{-11} , \tag{5}$$

$$SiH_4+OH \rightarrow SiH_3+H_2O \text{ with } k_5=1.3\times10^{-11} , \tag{6}$$

$$OH+OH \rightarrow H_2O+O(^3P) \text{ with } k_6=1.8\times10^{-12} , \tag{7}$$

$$H_2O+h\nu(185\text{ nm}) \rightarrow OH+H \text{ with } \sigma_2=5.54\times10^{-20} . \tag{8}$$

It must be pointed out that reaction (6) is about ten times as efficient as reaction (2) to dissociate silane at equal concentration of reactants. The presence of water in the films testifies for the importance of the OH-related reaction pathways.

It is true that a comprehensive picture of photodeposition will ask for the inclusion of more reactions. One of these involves the recombination of silyl radicals into disilane. Another more interesting set involves the creation of $SiOH_x$ species in the gas phase, which has recently been shown to play some part in low-pressure thermal deposition of silicon dioxide,[31] and which may lead to photonucleation of powdery silica germs in the gas phase in some form of polymerization reaction. Though we have chosen gas-flow parameters leading to deposition rates below the threshold for powdery deposits, which began in our experiments at silane flow values above 10 SCCM, we cannot completely exclude such processes from a realistic set of chemical reactions. Since this is beyond the scope of this work, we will only try to interpret our data from Eqs. (1)–(8).

They show that the dominant reactive species created by ultraviolet irradiation in the gas phase will be atomic oxygen $O(^3P)$, hydroxyl, and silyl radicals. It is then possible to build at two-step picture of silicon dioxide photodeposition. SiH_2 surface sites are quickly oxidized by atomic oxygen and OH groups, a process that leads to the production of water and hydroxyl groups at the surface and leave behind monohydrides which are less reactive than dihydride species. Impinging silyl molecules will then be incorporated in the film by losing one hydrogen on OH-related groups, thus leading to the creation of Si-O-Si bonds and dihydride SiH_2 groups at the deposition front. This reaction must also involve oxidization of the dangling bonds, since the study of these films by electron spin resonance did not show any paramagnetic signal.[32] The point is that the two-step qualitative description of silicon dioxide photodeposition falls under a general statistical model for deposition, which leads to definite predictions for the morphology of the films.

VIII. PHOTODEPOSITION AT LOW TEMPERATURES AND THE KPZ MECHANISM

In the two-step sequence described above incoming silyl and oxidizing radicals impinge on the surface to be incorporated in the film in a sequential manner. At temperatures as low as 20 °C, diffusion of chemisorbed species can be excluded so that one can assume the reaction to occur at the impact site, provided it contains the right chemical species, OH groups for incoming silyl radicals and dihydrides for oxidizing radicals. The mean free path of radicals in the gas phase is of the order of a few tens of microns, and the whole process can be viewed as ballistic aggregation with random incidence angles.[33] The evolution of the surface in such a process can be described by the Kardar-Parisi-Zhang (KPZ) equation, a nonlinear generalization of the Langevin equation leading to power-law roughening of the deposition front. It has been shown in this paper that a small part of the silicon atoms in the film is incorporated from silane in the gas phase striking photoexcited water on the surface. The statistical model describing such a mechanism is the Eden model, where sites on the surface are randomly activated (in this case by photoexcitation) for growth.[34] The Eden model can also be described by the KPZ formalism.[35] As a consequence, the photodeposition of silicon dioxide from silane-oxygen mixtures, even if a complex and composite process, should lead to power-law roughening of the deposition front with the characteristic exponent predicted by the KPZ model, for whom theoretical and numerical investigations have yielded values comprised between 0.20 and 0.33.[36]

It has been shown in this paper that adsorbed water and dihydrides were species characteristic of the active surface. The proportion of each type of site on the surface is characteristic of the chemical kinetics of gas-surface processes. For example, in preliminary experiments in SiO_2 photodeposition from silane and nitrogen protoxide mixtures, where the quantity of oxidizing species is less than in the silane-oxygen system, we have observed a higher amount of dihydride sites together with a much lower amount of adsorbed water. In the Fourier transform infrared experiments described above, we are able to follow the number of active surface species as a function of the amount of deposited material. Figure 9 plots such data for adsorbed water and dihydrides,

figuring a similar power-law dependence at room temperature with a characteristic exponent $\beta=0.28\pm0.05$. Finding the same evolution law for both species provides evidence that their relative ratio on the surface is constant, and that each set of data can characterize the evolution of the active surface width as a function of the amount of deposited material. The experimental determination of the kinetic roughening exponent β is in fair agreement with numerical and theoretical estimates deduced from the KPZ model, and ensures a self-consistency of our depiction of SiO_2 photodeposition from silane-oxygen mixtures. It makes photodeposition of silica films a relevant system to study experimentally deposition phenomena. It must indeed be pointed out that previous experimental studies have dealt with quasi-two-dimensional miscribility in porous media,[37] giving much higher exponents than theoretical predictions, possibly because of noise correlations.[38]

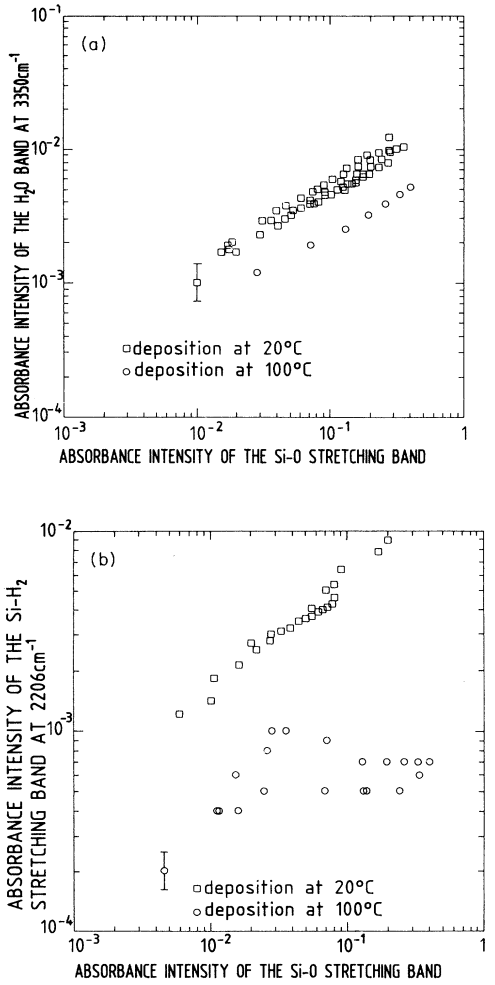

FIG. 9. (a) log-log plot of the absorbance intensity of the adsorbed water band vs intensity of the Si-O-Si stretching band, for deposition processes performed at room temperature and 100 °C. (b) log-log plot of the absorbance intensity of the dihydride stretching mode at 2208 cm^{-1} vs intensity of the Si-O-Si stretching band at deposition processes performed at room temperature and 100 °C.

It is both interesting and somewhat puzzling to consider what happens at moderately higher temperatures such as 100 °C. Figures 9(a) and 9(b) show the respective evolutions of the water and dihydride absorption bands at both temperatures. The water band is significantly lower by a factor of 4 than in room-temperature experiments, but it increases with the amount of deposited material in a similar power-law fashion. On the other hand, the dihydride absorption band which evolves very little during simple thermal annealing saturates very rapidly here at a constant value. A possible interpretation, for the definitive proof of which more work is needed, may start from the fact that dihydride sites are extremely reactive to oxidizing species, so that those observed in infrared spectroscopy are located on sites where they have long lifetimes for geometrical reasons, such as overhangs and pores. A power-law increase of the number of dihydride sites may then be characteristic of a ballistic process with a high degree of porosity in the deposit. Determination of the density in the deposits by glancing x-ray reflectivity indicates a density in the SiO_2 films made by UVCVD at room temperature lower than that of silica film obtained by thermal oxidation of silicon wafers by 20% to 30% according to the thickness of the deposited film.[39] When one raises the temperature, one may allow for diffusion and reorganization on a small finite scale, which will displace the deposition mode from ballistic towards random deposition with surface diffusion, leading towards a compact deposit with power-law roughening of the surface, which also evolves according to a power law.[40] The compactness of such deposits greatly limits the number of geometries preventing the oxidization of dihydride sites and allows for the observations of Fig. 9(b), that is a constant amount of dihydride sites in depositions performed above 100 °C. In this approach, the absorption signal due to adsorbed water which is much less reactive than the dihydride sites should be characteristic of the number of surface sites in each deposition mode. Indeed at higher temperatures where we have argued for more compact deposits from a random deposition model, this absorption band is significantly less intense, but keeps on increasing with the same exponent as that obtained at room temperature in a deposition mode we have argued to be similar to ballistic aggregation.

IX. CONCLUSIONS

We have studied the photochemical mechanisms involved in the UV-induced photodeposition of silica thin films from SiH_4/O_2 gaseous mixtures, by a surface sensitive infrared reflection-adsorption technique. With the help of this *in situ* technique, it has been possible to control deposition down to the monolayer range, for substrate temperatures between room temperature and 200 °C. A stretching Si-H absorption band at 2208 cm^{-1} has been identified as the characteristic surface molecular configuration resulting from silicon photoinduced incorporation into the film. By studying the spectra in the

low-energy region, a correlation of this stretching line has been made with a doublet structure at 975 and 935 cm^{-1}, which has been assigned to O_2SiH_2 bonding configurations. Incorporation of silane can occur by photogeneration of SiH_3 radicals in the gas phase in presence of oxygen, but our study has shown a second mechanism which occurs under UV irradiation without oxygen on the gas phase, which involves photoexcitation of adsorbed water and subsequent reaction with incoming silane molecules. Though this photoinduced mechanism accounts for only about 5% percent of silane incorporation in a normal deposition experiment, it is potentially useful because it is surface-controlled in the sense that it is limited by the availability of particular surface species, so that one may envision a step-by-step photodeposition of silica by successive exposures to oxygen and silane.

In the last part of our paper, we have studied the evolution of the absorption intensity due to specific surface molecular configurations, that is adsorbed water and dihydride species, as a function of deposited film thickness. At room temperature, both absorption bands increase according to a power law which is in fair agreement with the KPZ model for deposition. At 100 °C it is still the case for the absorbed water, though it is about four times less intense, but the amount of dihydride species rapidly saturate at a low value. This behavior might indicate an evolution in the porosity of the deposit, higher temperatures favoring small-scale diffusion which possibly leads to a compact film structure with a rugous deposition front, as is the case in random deposition model.

More work is clearly needed to completely elucidate the photodeposition of dielectric materials, but it must be noted that some achievements of this study, that is, providing direct evidence on surface sites involved in the deposition mechanism, and showing that silica photodeposition is a relevant experimental phenomenon for statistical growth models, can readily be extended with the same experimental methods to the photodeposition of silicon dioxide, nitride and oxynitrides from various chemical precursors: it is now possible to envision a systematic experimental study of these low-temperature photodeposition processes from a more fundamental point of view.

[1]M. Hanabusa, Mat. Sci. Rep. **2**, 51 (1987); H. Stafast, Appl. Phys. A **45**, 93 (1988), and references within.

[2]M. Okuyama, Y. Toyoda, and Y. Hamakawa, Jpn. J. Appl. Phys. **23**, L97 (1984); Y. Tarui, J. Hidaka, and K. Aota, *ibid.* **23**, L827 (1984); J. Takahashi and M. Tabe, *ibid.* **24**, 274 (1985); Y. I. Nissim, J. L. Regolini, D. Bensahel, and C. Licoppe, Electron. Lett. **24**, 488 (1988).

[3]P. K. Boyer, G. A. Roche, W. H. Ritchie, and G. J. Collins, Appl. Phys. Lett. **40**, 716 (1982); M. Petitjean, N. Proust, J. F. Chapeaublanc, and J. Perrin, Appl. Surf. Sci. **46**, 189 (1990).

[4]J. Marks and R. Robertson, Appl. Phys. Lett. **52**, 810 (1988).

[5]S. Otsubo, M. Saito, A. Moromoto, M. Kumeda, and T. Shimizu, Jpn. J. Appl. Phys. **27**, 1999 (1988).

[6]K. Inoue, M. Michimori, M. Okuyama, and Y. Hamakawa, Jpn. J. Appl. Phys. **26**, 805 (1987).

[7]H. Nonaka, K. Arai, Y. Fujino, and S. Ishimura, J. Appl. Phys. **64**, 4168 (1988).

[8]D. V. Tsu, G. Lucovsky, and B. N. Davison, Phys. Rev. B **40**, 1795 (1989).

[9]Y. J. Chabal, Surf. Sci. Rep. **8**, 211 (1988).

[10]F. Family and T. Vicsek, *Dynamics of Fractal Surfaces* (World Scientific, Singapore, 1991).

[11]Y. I. Nissim, J. M. Moison, F. Houzay, F. Lebland, C. Licoppe, and M. Bensoussan, Appl. Surf. Sci. **46**, 175 (1990).

[12]C. Licoppe, C. Debauche, F. Houzay, J. Flicstein, Y. I. Nissim, and J. M. Moison, Appl. Surf. Sci. **56-58**, 789 (1992).

[13]F. J. Himpsel, F. R. McFeely, A. Taleb-Ibrahimi, J. A. Yarmoff, and G. Hollinger, Phys. Rev. B **38**, 6064 (1988); F. R. McFeely, E. Cartier, J. A. Yarmoff, and S. A. Joyce, *ibid.* **42**, 5191 (1991).

[14]D. C. Paine, J. J. Rosenberg, S. C. Martin, D. Luo, and M. Kawazaki, Appl. Phys. Lett. **57**, 1443 (1990).

[15]C. Licoppe, C. Meriadec, J. Flicstein, Y. I. Nissim, and A. C. Papadopoulo, Appl. Phys. Lett. **59**, 43 (1991).

[16]C. T. Kirk, Phys. Rev. B **38**, 1255 (1988); P. Lange, J. Appl. Phys. **66**, 201 (1989).

[17]G. Lucovsky, Solid State Commun. **29**, 571 (1979).

[18]C. Licoppe, F. Wattine, C. Meriadec, J. Flicstein, and Y. I. Nissim, J. Appl. Phys. **68**, 5636 (1990).

[19]K. H. Beckmann and N. J. Harrick, J. Electrochem. Soc. **118**, 614 (1971); W. R. Knolle, H. R. Maxwell, and R. E. Benenson, J. Appl. Phys. **51**, 4385 (1980).

[20]D. V. Tsu, G. Lucovsky, and B. N. Davidson, Phys. Rev. B **40**, 1795 (1989).

[21]W. B. Pollard and G. Lucovsky, Phys. Rev. B **26**, 3172 (1982).

[22]J. Flicstein, Y. I. Nissim, C. Licoppe, and Y. Vitel, French patent No. 9103964 (pending).

[23]Y. Harada, J. N. Murrell, and H. Sheena, Chem. Phys. Lett. **1**, 595 (1968); R. Roberge, C. Sandorfy, J. I. Matthews, and O. P. Strausz, J. Chem. Phys. **69**, 5105 (1978); M. Suto and L. C. Lee, *ibid.* **84**, 1160 (1984).

[24]B. S. Agrawalla and D. W. Setser, J. Chem. Phys. **86**, 5421 (1987); C. R. Park, G. D. White, and J. R. Wiesenfeld, *ibid.* **92**, 152 (1988); S. Koda, S. Tschuchiya, T. Suzuki, C. Yamada, and E. Horota, Chem. Phys. Lett. **161**, 152 (1988).

[25]G. W. Stephenson and K. H. Jack, Trans. Brit. Ceram. Soc. **59**, 397 (1960); A. J. Moulson and J. P. Roberts, Trans. Faraday. Soc. **57**, 1208 (1961).

[26]H. Okabe, *Photochemistry of Small Molecules* (Wiley, New York, 1978).

[27]C. Licoppe, C. Meriadec, J. Flicstein, Y. I. Nissim, and A. C. Papadopoulo, Appl. Phys. Lett. **59**, 43 (1991).

[28]M. Nakano, H. Sakaue, H. Kawamoto, A. Nagata, M. Hirose, and Y. Horiike, Appl. Phys. Lett. **57**, 1096 (1990); D. J. Ehrlich and J. Melngailis, *ibid.* **58**, 2675 (1991).

[29]D. L. Baulch, CODATA Task Group, J. Phys. Chem. Ref. Data **2**, 181 (1982).

[30]Y. Tarui, J. Hidaka, and K. Aota, Jpn. J. Appl. Phys. **23**, L827 (1984).

[31]P. Van de Weijer and B. H. Zwerver, Chem. Phys. Lett. **163**, 48 (1989); M. Liehr and S. A. Cohen, Appl. Phys. Lett. **60**,

198 (1992).
[32]C. Debauche, C. Licoppe, J. Flicstein, and R. A. B. Devine, Appl. Phys. Lett. **61(3)**, 306 (1992).
[33]P. Meakin, P. Ramanlal, L. M. Sander, and R. C. Ball, Phys. Rev. A **34**, 5091 (1986); P. Meakin and R. Jullien, Physica A **175**, 211 (1991).
[34]M. Eden, in *Proceedings of the Fourth Berkeley Symposium on Mathematical Statistics and Probability,* edited by F. Neyman (University of California, Berkeley, CA, 1981), Vol. 4, p. 223.
[35]M. Kardar, G. Parisi, and Y. C. Zhang, Phys. Rev. Lett. **56**, 889 (1986).
[36]J. G. Zabolitzky and D. Stauffer, Phys. Rev. A **34**, 1523 (1986); D. E. Wolf and J. Kertesz, Europhys. Lett. **4**, 651 (1987); J. Kertesz and D. E. Wolf, J. Phys. A **21**, 747 (1988); J. M. Kim and J. M. Kosterlitz, Phys. Rev. Lett. **62**, 2289 (1989); F. Family, Physica A **168**, 561 (1990).
[37]M. A. Rubio, C. A. Edwards, A. Dougherty, and J. P. Gollub, Phys. Rev. Lett. **63**, 1685 (1989); V. K. Horvath, F. Family, and T. Vicsek, J. Phys. A **24**, L25 (1991).
[38]E. Medina, T. Hwa, M. Kardar, and Y-C. Zhang, Phys. Rev. A **39**, 3053 (1989); Y-C. Zhang, J. Phys. **51**, 2129 (1990); J. G. Armar, P-M. Lam, and F. Family, Phys. Rev. A **43**, 4548 (1991).
[39]J. J. Benattar (private communcation).
[40]F. Family, Physica A **168**, 561 (1990).